CREEP CRACK GROWTH IN NIMONIC 80A AND IN A 1CR-1/2MO STEEL

H. Riedel and W. Wagner

Max-Planck-Institut fuer Eisenforschung, Max-Planck-Str. 1, 4000 Duesseldorf, Federal Republic of Germany

ABSTRACT

Creep crack growth rates have been measured in the nickel-base alloy Nimonic 80A at 600°C and 650°C and in a 1Cr-1/2Mo steel at 450°C, 535°C and 600°C in air and in Ar/3%H_2. In Nimonic 80A, the crack growth rates correlate with the stress intensity factor K_I, while in the steel, the line integral C^* has been found to be the correlating load parameter. Both observations are in accord with continuum-mechanical theories of creep crack growth. The micromechanism of crack extension in Nimonic 80A could not be clarified conclusively. Corrosive effects certainly play a role as demonstrated by the sensitivity to the atmosphere. Crack growth in the steel is quantitatively described by a model based on creep-constrained cavitation of grain boundaries ahead of the crack tip. Several other possibilities can be ruled out.

KEYWORDS

Creep crack growth, fracture mechanics at high temperature, creep cavities.

INTRODUCTION

Crack growth under elevated temperature creep conditions has two important aspects. The first aspect concerns the macroscopic deformation behavior of the cracked specimen. A continuum-mechanical analysis of the deformation fields answers the question which load parameter (K_I,J, C^* etc.) characterizes the crack-tip fields. Such an analysis has been done by Riedel and Rice (1980), Ohji et al (1980a) and Riedel (1981a). The micromechanisms of crack extension (grain-boundary cavitation, corrosion) represent the second aspect of creep crack growth. Both of these aspects will be addressed below by comparing theoretical predictions with data obtained for two commercial alloys.

EXPERIMENTAL

The γ'- hardened nickel base alloy NIMONIC 80A was received as a forged bar which was given the standard two-step heat treatment. The alloying elements

were 19%Cr, 2.2%Ti, 1.3%Al, 0.28%Fe, 0.18%Si, 0.13%Mn and 0.07%C. The creep rate in uniaxial tension can be fitted with Norton's creep law

$$\dot{\varepsilon} = A\,\sigma^n \qquad (1)$$

giving $A = 3.3\cdot10^{-44}$ MPa^{-n}/s and n=13 at 650°C. The 1Cr-1/2Mo steel (13CrMo44 in German notation) was tested as new material cut from a thick-walled pipe having a fine, bainitic microstructure. However, the majority of the tests was done on the same steel that had been in service for 103,000 h at 530°C under a stress of nominally 52 MPa. During that time, the carbides have coarsened and the uniaxial creep resistance has dropped accordingly. The parameters of Norton's creep law are $A = 5.6\cdot10^{-26}$ MPa^{-n}/s and n = 8.6 for the old material at 535°C.

Compact specimens were machined from these materials in the sizes CT1/2, CT1 and CT2. The specimens were pre-cracked by fatigue loading at room temperature and most of them had side grooves of the type suggested by the three-dimensional finite element calculations of deLorenzi and Shih (1983). Their depth is 25% of the half specimen thickness, the included notch angle is 45° and the notch root radius is 0.1 mm. These side-grooves should make the crack-tip field similar to the plane-strain field along the whole crack front. Accordingly, the crack front remained straight in side-grooved specimens except for a slight acceleration near the side grooves. To avoid this disturbance it is recommended to make the notch root a little less sharp.

The creep crack growth tests were done using servo-mechanical testing machines. A microprocessor controls the value of the force according to a desired program (e.g. constant K_I or C^*). Most of the tests reported here were done under constant load since K_I or C^* vary slowly enough so that there is no difference in crack growth rate compared to tests with constant K_I or C^*.

The crack length is measured using the electric potential drop technique and the elastic compliance. The potential drop technique, if compensated for temperature fluctuations, works well in the case of the steel but gives no reproducible signal for Nimonic 80A. As the reason for this we identified metallic bridges between the crack faces far behind the crack front. In Nimonic 80A at 650°C the crack advances with little ductility so that the separation of the crack faces is less than the roughness of the fracture surface. The compliance method allowed no precise crack length measurement either. One of the problems was the mechanical instability of the testing machine which experienced uncontrollable small torsions when the direction of the strain rate was reversed. Therefore, the crack length in Nimonic 80A was measured by markings on the fracture surface set by changes of the load or of the atmosphere. The potential drop technique and the compliance method were used to interpolate between the markings.

Different gases could be brought to the crack-tip region through a thin tube wound around the CT-specimens, following the machined notch and the side grooves. The tube contains fine holes towards the CT-specimen. This simple set-up suffices to set markings on the fracture surface and to test qualitatively whether creep crack growth is sensitive to the atmosphere. A strong corrosive effect has been reported to exist in many alloys (Speidel, 1981).

The C^*-integral was determined from load, P, load-line displacement rate, $\dot{\Delta}$, and crack length, a, according to the formulas given for J in the Fracture Handbook of Kumar et al (1981). (Recall that C^* is the viscous analogue of J if strain and displacement are replaced by their time rates). The following formulas were employed:

$$C^* = a\,A\,\sigma_{eff}^{n+1}\,g_1 = g_2\,\sigma_{eff}\,\dot{\Delta} = g_3\,\dot{\Delta}^{1+1/n}(aA)^{-1/n}, \qquad (2)$$

where the g's are functions of the ratio a/W (W = specimen width) and of the creep stress exponent n. Their relation to the functions h_1, h_2, h_3 tabulated by Kumar et al (1981) is obvious and has been explicitly given by Riedel (1983a). For specimens without side grooves, σ_{eff} is the net section stress, σ_{net}, (load/area of ligament). Side grooves are taken into account in the usual approximate manner by using the plane-strain values for g_1, g_2, g_3 and writing

$$\sigma_{eff} = P/[(W-a)B_{eff}] \quad \text{with} \quad B_{eff} = B - (B-B_{net})^2/B. \qquad (3)$$

Here, B is the total specimen thickness and B_{net} is the thickness between the roots of the side grooves. The forms of eq. (2) containing $\dot{\Delta}$ can only be applied if the displacement rate, $\dot{\Delta}$, arises mainly from creep deformation of the specimen rather than from the increasing elastic compliance by crack growth. This requirement is fulfilled for the steel but not for Nimonic 80A in our experiments.

THE APPROPRIATE LOAD PARAMETER

If the deformation behavior of the material (with the possible exception of a small zone near the crack tip) can be described as elastic-nonlinear viscous, cracked specimens exhibit a transient deformation behavior from predominantly elastic to extensive creep. The characteristic time for this transition has been calculated by Riedel and Rice (1980) and by Ohji et al (1980a) as

$$t_1 = K_I^2(1-\nu^2)/[(n+1)E\,C^*] \qquad (4)$$

(ν is Poisson's ratio). As an example, consider two CT1-specimens with a/W = 0.5 without side grooves, one made of Nimonic 80A and the other made of the old material of the CrMo steel. The first one is subjected to a load 30 kN at 650°C and the second one to 22 kN at 535°C. With the creep data given in the section on Experimental, C^* can be calculated from the first form of eq. (2), while K_I is determined in the usual way. Taking E = 170 GPa for the nickel alloy and E = 150 GPa for the steel gives t_1 = 600 years for the nickel alloy

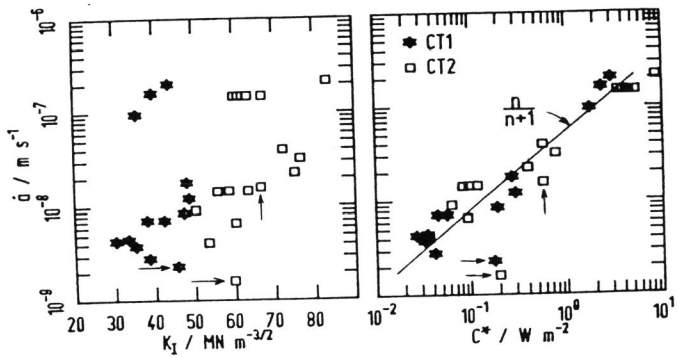

Fig. 1. Correlation of crack growth rate with K_I and C^* for new material of 1Cr-1/2Mo steel at 535°C. Arrows denote data near beginning of tests.

and t_1 = 26 minutes for the steel specimen. Since under the conditions assumed, the lifetime of the two specimens is found experimentally to be a few weeks, it is clear that the Nimonic specimen fails within the elastically dominated short-time limit, where K_I is the right load parameter, while the steel specimen fails within the C^*-controlled long-time limit.

Figure 1 demonstrates that in fact the crack growth rates measured in steel specimens of different sizes are uniquely described by C^*, whereas K_I gives no reasonable correlation. The correlation of the crack growth rate, $\dot{a}$, with K_I for Nimonic 80A is shown in Fig. 3. Of course, K_I can only correlate the data points measured at the same temperature in the same environment. The correlation is not overwhelming, maybe due to the experimental difficulties described above, but it were much worse if C^* had been used.

MICROMECHANISMS AND CRACK GROWTH RATES

In Nimonic 80A, cracks grow intergranularly. Parts of the fracture surface show the dimpled structure which is typical for grain-boundary cavitation. On etched and polished sections of the crack-tip region, cavities could only rarely be identified, and it is not obvious by which micromechanism a sharp crack like that shown in Fig.2 manages to separate the grains, preferably along the carbide/matrix interface. In the optical microscope, the grain-boundary carbides near the crack tip look as though they were affected by corrosion. At any rate, corrosive effects play an important role in Nimonic 80A. This is demonstrated in Fig. 3, which shows that crack growth rates in argon + 3% hydrogen are about ten times greater than in air. The data points for 650°C in air suggest a bilinear dependence of $\dot{a}$ on K_I (in a log-log plot). At high values of K_I, the slope is between 4 and 5 while at low stresses the data are compatible with a slope of 13. A slope equal to the creep stress exponent, n=13, is expected if crack growth ensues subject to a critical strain criterion (Nix et al, 1977, Hui and Riedel, 1981). If the crack growth rate, $\dot{a}$, is assumed to depend on temperature in the usual exponential fashion, the data in Fig. 3 give an activation energy of 240 to 300 kJ/mole. Finally, the crack growth rate exhibits a transient behavior: shortly after the beginning of a test, the growth rates are higher than later on (for the same value of

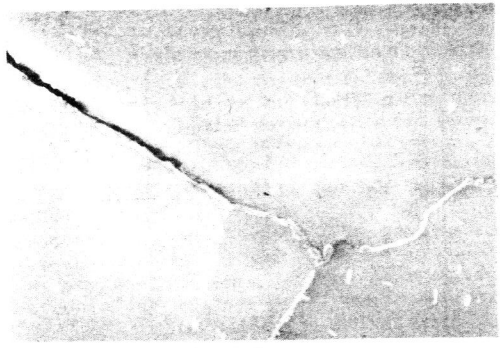

Fig. 2. The sharp tip of an intergranular crack in Nimonic 80A.

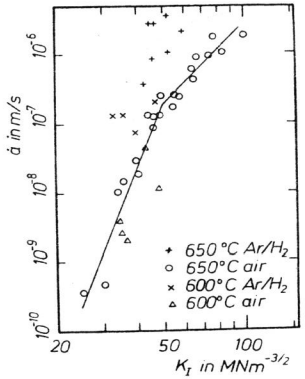

Fig. 3. Crack growth rate vs. K_I in Nimonic 80A.

K_I). For clarity's sake, these data points were omitted from Fig. 3. A consistent explanation for all these observations is not available.

For the chromium-molybdenum steel, the situation is much more favorable. Micrographs show grain boundary cavitation ahead of the crack tip as demonstrated by Fig. 4. The atmosphere (air or Ar/H_2) has no measurable effect on the crack growth rates. Correspondingly, the observed crack growth behavior can be explained successfully by a model for crack extension by coalescence with cavities (Riedel, 1981b, 1983a). If local failure by cavity coalescence is controlled by the attainment of a critical strain, ε_c, over a microstructural length, x_c, the main crack starts growing after an incubation time

$$t_i = (1/\alpha_n') \, (1+1/n) \, \varepsilon_c \, (x_c/C^*)^{n/(n+1)}/A^{1/(n+1)}. \qquad (5)$$

Direcly after initiation, the crack grows at a rate $\dot{a}_i = x_c(1+1/n)/t_i$ while for larger amounts of growth, $\Delta a \gg x_c$, the growth rate becomes

$$\dot{a} = \alpha_n \, A^{1/(n+1)} \, C^{*n/(n+1)} \, [\Delta a^{1/(n+1)} - \beta_n \, x_c^{1/(n+1)}]/\varepsilon_c. \qquad (6)$$

The numerical constants have typical values of $\alpha_n = 0.046$, $\alpha_n' = 0.0052$, $\beta_n = 0.96$ for n = 8.6, and $\alpha_n = 0.043$, $\alpha_n' = 0.0060$, $\beta_n = 0.94$ for n = 7. For creep-constrained cavity growth, ε_c is of the order

$$\varepsilon_c = 0.3(\sigma_e/\sigma_I) \, x_c/d = 0.08 \, x_c/d, \qquad (7)$$

where d is grain size (Dyson, 1976, Rice, 1981, Riedel, 1983b). Here, the numerical factors are valid for n = 8.6. In the second form, the ratio between equivalent tensile stress and maximum principal stress was chosen as 0.26 as appropriate for the HRR-field of a plane-strain crack. Taking $x_c/d = 1/20$ gives a critical strain of 0.4%.

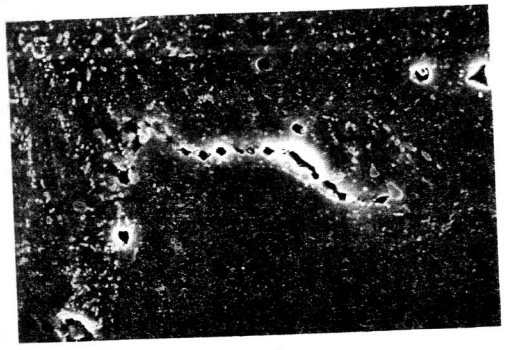

Fig. 4. Cavitation ahead of main crack in 1Cr-1/2Mo steel (old material) tested at 535°C. Tensile direction is vertical.

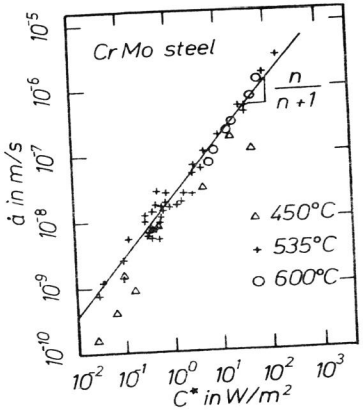

Fig. 5. Crack growth rate in 1Cr-1/2Mo steel (old material) in air and in Ar/H_2.

The measured crack growth rates shown in Figs. 1 and 5 agree very well with the rates predicted by eq. (6): The dependence on C^* has the expected power-law form with the exponent $n/(n+1)$. The temperature dependence is found to be moderate. This agrees with eq. (6), where the temperature enters through the creep coefficient, A, raised to the small power $1/(n+1)$. If ε_c is taken as a fittable parameter to fit eq. (6) to the data in Fig. 5, it results that $\varepsilon_c = 0.7\%$ which is exactly the order of magnitude expected for creep-constrained cavitation. For this fit, $\Delta a = 3$ mm and $x_c = 2$ μm were chosen. The value obtained for ε_c is insensitive to the choice of these quantities. Fig. 1 also shows a few data points that were measured near the start of creep crack extension. They lie consistently below the scatterband of the other data. This also agrees with the theory, which predicts that the initial growth rate is by a factor 5 to 10 smaller than the rate after a few millimeters of crack extension, for the same value of C^*. Thus the transient behavior of $\dot{a}$ in the steel is just opposite to that in Nimonic 80A. The incubation time for crack growth initiation follows from eq. (5) to be $t_i = 20$ minutes taking $\varepsilon_c = 0.7\%$, $x_c = 2$ μm, and $C^* = 1$ W/m^2. Such a short time plays no role compared with the lifetime of the cracked specimen. No attempt was made to measure t_i.

DISCUSSION

Creep crack growth in the chromium-molybdenum steel has been described consistently by a model based on creep-constrained cavity growth ahead of the main crack. On the other hand, Riedel (1981b) has shown that cavity growth by grain boundary diffusion combined with easy cavity nucleation leads to a completely different dependence of $\dot{a}$ on C^* and temperature, which cannot be reconciled with the observed behavior. However, Hui and Banthia (1983) and the present authors observed independently that the experimental data can also be explained (except for a quantitative point as we shall see) if cavity nucleation is taken into account in conjunction with diffusional cavity growth. To explore this point we assume that the macroscopic stress field of the crack is the well-known HRR-field. Further, let cavities nucleate at discrete nucleation sites once the tensile stress exceeds the nucleation stress, σ_n (Raj, 1978), which will be treated as a fittable parameter. The law for diffusional cavity growth is taken, for example, from Needleman and Rice (1980). The main crack grows by coalescence with the cavities. This implies that the crack must grow at such a rate that the cavities directly ahead of its tip had enough time to grow to a size equal to their spacing in the HRR-field of the approaching main crack. For simplicity, the sintering stress in the cavity growth law is neglected, the function $h(\psi)$ is given the value 0.61, and the cavity size at nucleation is neglected against the cavity spacing. Then an analysis parallelling that by Riedel (1981b) gives the crack growth rate. In the steady state, especially, the growth rate is

$$\dot{a} = 250\,\frac{\Omega\delta D_b}{kTx_c^3}\,\frac{n+1}{n}\left(\frac{C^*}{I_n A}\right)^{1/(n+1)} \tilde{\sigma}_{22}(0)\,\left[(r_n+x_c)^{n/(n+1)} - x_c^{n/(n+1)}\right] \qquad (8)$$

with Ω = atomic volume, δD_b = grain boundary diffusion coefficient, k = Boltzmann's constant, x_c = cavity spacing. The constants I_n and $\tilde{\sigma}_{22}(0)$ characterize the HRR-field and have the values $I_n = 4.63$ and $\tilde{\sigma}_{22}(0) = 2.44$ for $n = 8.6$. Further, r_n is the distance ahead of the crack over which the HRR-field exceeds the cavity nucleation stress. It is related to the nucleation stress by $r_n = (C^*/I_n A)\,(\tilde{\sigma}_{22}(0)/\sigma_n)^{n+1}$. Substituting this into eq. (8) and neglecting x_c against r_n gives the crack growth rate

$$\dot{a} = [250(1+1/n)\tilde{\sigma}_{22}^{n+1}/I_n]\;\Omega\,\delta D_b\,C^*/(kT\,x_c^3\,A\,\sigma_n^n), \qquad (9)$$

where the factor in square brackets is $3\cdot10^5$ for $n = 8.6$.

The linear dependence of $\dot{a}$ on C^* predicted by eq. (9) above is compatible with the experimental data. Further, the temperature dependence of $\dot{a}$ is primarily determined by the ratio $\delta D_b/A$. Since the creep coefficient A generally has a greater activation energy than δD_b, eq. (9) predicts a crack growth rate which decreases for increasing temperature. The experiments in Fig. 5 indicate the opposite trend, although both, the observed and predicted temperature dependences are weak. Thus the result appears to be roughly compatible with experiments at first sight. However, r_n can be considered as a fittable parameter in eq. (8), while $\dot{a}$ and C^* are taken from Fig. 5, and Ω and δD_b are taken from the tabulations of Frost and Ashby (1977). For T = 808 K, $\dot{a} = 10^{-8}$ m/s, $C^* = 0.5$ W/m^2 and $x_c = 3$ μm, the result is $r_n = 14$ m. (The corresponding nucleation stress, which is of no interest in the following, is then $\sigma_n = 150$ MPa). The large value of r_n implies that in our tests cavity nucleation would have occurred immediately in the whole specimen. Hence we must return to the theory with easy nucleation. In conclusion, diffusional cavity growth in conjunction with cavity nucleation cannot explain our experimental data.

The present experimental results broadly agree with the observations of other workers. Ohji et al (1980b) demonstrate the applicability of K_I or C^*, respectively, for a variety of steels. Taira et al (1979) find the same qualitative dependence of the crack growth rate on C^*, on temperature and on the crack growth increment for several ferritic and austenitic steels as we do for the CrMo steel. Of course, the limitations to the approach which works so well in many instances must be explored if it is to be applied safely to practical problems. Saxena et al (1984), for example, observe poor correlation of crack growth rates in a stainless steel with C^*, and good correlation with the J-integral. Their tests, however, have been done at rather high load levels and correspondingly short life times so that indeed instantaneous plasticity, and therefore J, should determine the macroscopic response of the specimen as pointed out by Riedel (1983a).

CONCLUSIONS

(1) Creep crack growth in Nimonic 80A at 600°C and 650°C can be described macroscopically by the stress intensity factor over a wide range of stresses.
(2) If the growth rate is written as $\dot{a} \propto K_I^m$, the exponent m is found to range from around 13 to 4 at 650°C in air.
(3) The temperature dependence of $\dot{a}$ in Nimonic 80A for constant K_I is described by an activation energy between 240 and 300 kJ/mole.
(4) Creep crack growth in Nimonic 80A is sensitive to the atmosphere. Cracks grow ten times faster in Ar/H_2 than in air.
(5) In a 1Cr-1/2Mo steel, C^* was found to be the appropriate load parameter in accord with theoretical predictions.
(6) The growth rate depends weakly on temperature (for constant C^*) and varies as $\dot{a} \propto C^{*n/(n+1)}$.
(7) These dependencies can consistently be explained by a micromechanistic model based on creep-constrained cavitation of grain boundaries ahead of the crack tip. Even the absolute values of $\dot{a}$ are predicted correctly to within a factor of 2.
(8) A competing model based on diffusional cavity growth and stress-controlled cavity nucleation fails to predict the observed behavior consistently.
(9) The material that had been in service for 103,000 h shows no faster crack growth than the new material, although the uniaxial data differ significantly.

Acknowledgement. Financial support from the Deutsche Forschungsgemeinschaft under contract No. Ri 329/8-2 is gratefully acknowledged.

REFERENCES

deLorenzi, H.G. and Shih, C.F. (1983). Int. J. Fracture, 21, 195-226.
Dyson, B.F. (1976). Metal Sci., 10, 349-353.
Frost, H.J. and Ashby, M.F. (1977). Deformation-Mechanism Maps for Pure Iron, Two Austenitic Stainless Steels and a Low-Alloy Ferritic Steel. In: R.I. Jaffee and B.A. Wilcox (Eds.), Fundamental Alloy Design, Plenum Press, New York and London, pp. 27-58.
Hui, C.Y. and Banthia, V. (1983). Private communication. Work in progress.
Hui, C.Y. and Riedel, H. (1981). Int. J. Fracture, 17, 409-425.
Kumar, V., German, M.D. and Shih, C.F. (1981). An Engineering Approach for Elastic-Plastic Fracture Analysis, EPRI-Report NP-1931, Palo Alto.
Needleman, A. and Rice, J.R. (1980). Acta Metall. 28, 1315-1332.
Nix, W.D., Matlock, D.K. and Dimelfi, R.J. (1977). Acta Metall., 25, 495-503.
Ohji, K., Ogura, K. and Kubo, S. (1980a). J. Soc. Mater. Sci. Japan,29, No. 320,465-471.
Ohji, K., Ogura, K., Kubo, S. and Katada, Y. (1980b). The Application of Modified J-Integral to Creep Crack Growth. In: Engineering Aspects of Creep, Vol. 2, The Institution of Mechanical Engineers, London, 9-16.
Raj, R. (1978). Acta Metall., 26, 995-1006.
Rice, J.R. (1981). Acta Metall., 29, 675-681.
Riedel, H. (1981a). J. Mech. Phys. Solids, 29, 35-49.
Riedel, H. (1981b). The Extension of a Macroscopic Crack at Elevated Temperature by the Growth and Coalescence of Microvoids. In: A.R.S. Ponter and D.R. Hayhurst (Eds.), Creep in Structures, Springer Verlag, Berlin Heidelberg New York, pp. 504-519.
Riedel, H. (1983a). The Use and the Limitations of C^* in Creep Crack Growth Testing. In: Tan Deyan and Chen Daning (Eds.), International Symposium on Fracture Mechanics, Science Press, Beijing, China, pp. 997-1012.
Riedel, H. (1983b). Constrained Grain Boundary Cavitation in a Creeping Body Containing a Macroscopic Crack. In: J. Carlsson and N.G. Ohlson (Eds.), Mechanical Behaviour of Materials, (ICM4), Vol. 1, Pergamon Press, Oxford, pp. 67-78.
Riedel, H. and Rice, J.R. (1980). Tensile Cracks in Creeping Solids. In: P.C. Paris (Ed.), Fracture Mechanics: Twelfth Conference, ASTM STP 700, American Society for Testing and Materials, pp. 112-130.
Saxena, A., Ernst, H.A. and Landes, J.D. (1984). Submitted to Int. J. Fracture. Also available as Scientific Paper 82-1D7-REACT-P1, Westinghouse R and D Center, 1310 Beulah Road, Pittsburgh, 1982.
Speidel, M.O. (1981). Influence of Environment on Fracture. In: D. Francois et al (Eds.), Advances in Fracture Research, Vol. 6, (ICF5), Pergamon Press, Oxford, pp. 2685-2704.
Taira, S., Ohtani, R. and Kitamura, T. (1979). J. Eng. Mater. Technology, 101, 154-161.